

**THE UNIVERSITY OF MANCHESTER - APPROVED ELECTRONICALLY  
GENERATED THESIS/DISSERTATION COVER-PAGE**

Electronic identifier: 18118

Date of electronic submission: 29/04/2016

The University of Manchester makes unrestricted examined electronic theses and dissertations freely available for download and reading online via Manchester eScholar at <http://www.manchester.ac.uk/escholar>.

This print version of my thesis/dissertation is a TRUE and ACCURATE REPRESENTATION of the electronic version submitted to the University of Manchester's institutional repository, Manchester eScholar.

# DEVELOPMENT OF PREDICTIVE FINITE ELEMENT MODELS FOR COMPLETE CONTACT FRETTING FATIGUE

A thesis submitted to the University of Manchester  
for the degree of  
Doctor of Philosophy (PhD)  
in the Faculty of Engineering and Physical Sciences

2015

MOHAMAD HAIDIR MASLAN  
School of Mechanical, Aerospace and Civil Engineering

## Table of Content

Table of Content.....	2
List of Figures .....	6
List of Tables.....	10
Abstract .....	11
Declaration .....	12
Copyright Statement .....	13
Acknowledgements .....	14
Nomenclature .....	15
CHAPTER 1. Introduction.....	18
1.1 Introduction .....	18
1.2 Fretting Fatigue .....	21
1.3 Previous Research .....	22
1.4 Overall Aim and Objectives .....	23
1.5 Structure of report .....	23
CHAPTER 2. Parameters in fretting fatigue.....	25
2.1 Introduction .....	25
2.2 Contact Mechanics .....	25
2.3 Tribology.....	29
2.3.1 Friction .....	29
2.3.2 Wear .....	30
2.4 Fatigue.....	32
2.4.1 Crack initiation.....	32
2.4.2 Linear Elastic Fracture Mechanics(LEFM) .....	35
2.4.3 Elastic Plastic Fracture Mechanics (EPFM) .....	40
2.4.4 Fatigue Crack Growth .....	41
2.5 Fretting Fatigue .....	42
2.6 Fretting Fatigue Experimental Test and Modelling .....	43

2.6.1 Fretting Pad Configuration.....	44
2.6.2 Fretting Contact Types.....	45
2.6.3 Other configurations.....	46
CHAPTER 3. Literature Review.....	48
3.1 Introduction.....	48
3.2 Crack Initiation.....	48
3.2.1 Friction evolution.....	49
3.2.2 Wear.....	49
3.2.3 Plastic Deformation.....	54
3.2.4 Other factors which affect crack initiation.....	56
3.2.5 Fretting Fatigue Crack Initiation Prediction.....	56
3.3 Early Crack Propagation.....	58
3.3.1 Propagation.....	58
3.3.2 Crack Direction.....	59
3.4 Crack Propagation and Final Failure.....	61
CHAPTER 4. Review of Previous Experimental work.....	62
4.1 Introduction.....	62
4.2 Experimental Setup and Specimen Geometry.....	62
4.3 Material Properties.....	63
4.4 Experimental Parameters.....	64
4.5 Experimental Results.....	65
4.5.1 Coefficient of Friction.....	65
4.5.2 Fretting Fatigue Life.....	66
4.5.3 Crack Propagation.....	66
4.5.4 Crack Path.....	71
4.6 Conclusions.....	73
CHAPTER 5. Model Development for Fretting Fatigue Life Prediction.....	74
5.1 Research Framework.....	74

5.2 Crack Initiation.....	76
5.2.1 Contact Friction Model Development.....	76
5.2.2 Wear Model Development .....	77
5.2.3 Critical Plane Damage Model .....	78
5.2.4 Averaging Method .....	79
5.3 Early Crack Growth Modelling.....	81
5.3.1 Crack Orientation .....	81
5.3.2 Crack Propagation.....	82
5.4 Stable Crack Growth and Final Fracture Modelling .....	83
CHAPTER 6. Crack Initiation in Complete Contact fretting fatigue .....	85
6.1 Introduction .....	85
6.2 Model Description.....	85
6.3 Validation of finite element model against theory .....	88
6.4 Results .....	89
6.4.1 Linear elastic analysis .....	89
6.4.2 Elastic Plastic Analysis .....	92
6.4.3 Wear Analysis .....	98
6.5 Averaging Method .....	100
6.6 Conclusion .....	103
CHAPTER 7. Crack Propagation in Complete Contact Fretting Fatigue.....	104
7.1 Introduction .....	104
7.2 Model Description.....	104
7.3 Crack path in complete contact fretting fatigue .....	105
7.3.1 Crack Propagation Analysis.....	107
7.3.2 Analysis with single edge and double edge cracks .....	120
7.4 Total Lifetime Prediction .....	121
7.5 Conclusions .....	122
CHAPTER 8. Conclusions and Future Work .....	123

8.1 Conclusions .....	123
8.1.1 Crack Initiation Analysis .....	123
8.1.2 Crack Propagation analysis .....	124
8.2 Recommendation for Future Work .....	125
Appendix 1: User Subroutine.....	127
Appendix 2 Abaqus Contact Modelling.....	130
Appendix 3: Effect of Plastic Deformation and Wear on Contact Pressure Profile .....	134
Appendix 4: Publications .....	139
References .....	148

## List of Figures

Figure 1.1: Fuselage fragment of Comet [2].	18
Figure 1.2: Aloha Airline flight 243 accident [3].	19
Figure 1.3: Schematic view of a countersunk rivet and the associated fatigue crack observed in Aloha Airlines 737 accident [3].	20
Figure 1.4: Photograph of Southwest airliner with a hole in the upper left fuselage [4].	20
Figure 1.5: Close-up view of the hole in the fuselage side skin [4].	21
Figure 1.6: fretting fatigue on (a) spline coupling (b) dovetail joint.	22
Figure 2.1: Various types of contact (a) Incomplete and non-conformal (b) Incomplete and conformal (c) Complete (d) Receding [6].	25
Figure 2.2: Schematic of 2D Hertzian contact.	26
Figure 2.3: Pressure distribution based on Hertz equation.	27
Figure 2.4: Punch on flat contact configuration.	28
Figure 2.5: Pressure distribution for a rigid, frictionless punch on a flat elastic half-space.	29
Figure 2.6: Illustration of the irreversibility of slip: formation of a microscopic hills and valleys on the surface of a material loaded in fatigue.	33
Figure 2.7: Schematic diagram of Strain Life curve [13].	34
Figure 2.8: Crack loading modes: Mode I, opening; mode II, sliding; mode III, tearing.	36
Figure 2.9: Definition of the coordinate axes and the stress field ahead of a crack tip in (a) cartesian coordinates, (b) polar coordinates.	36
Figure 2.10: Plastic zone size estimation based on Irwin postulate.	39
Figure 2.11: Arbitrary contour around the tip of a crack.	41
Figure 2.12: Fatigue Crack Growth Plot.	42
Figure 2.13: Schematic of a typical bridge-type experimental setup.	44
Figure 2.14: Schematic of a typical single fretting pad experimental setup.	45
Figure 2.15: Dovetail fretting fatigue experimental configuration [34].	46
Figure 2.16: Schematic of multiaxial representative specimen for spline coupling [30].	47
Figure 3.1: Schematic representation of the different stages of fretting fatigue crack initiation, propagation, and final failure [36].	48
Figure 3.2: Schematic of Adhesive Wear.	50
Figure 3.3: Schematic of Abrasive Wear.	50
Figure 3.4: Fretting wear (a) scar and (b) etched cross sectional view at line AA [46].	51

Figure 3.5: SEM images of a cross-section of the flat specimen [49].	52
Figure 3.6: Comparison of Archard Equation based fretting wear predictions and experimental wear scars for three increasing normal loads [39].	53
Figure 3.7: Physical model of damage development in bending fretting fatigue.	55
Figure 3.8: The SWT parameter against number of cycles to initiation [66].	57
Figure 3.9: Comparison of crack propagation trajectories given by MTS, MERR, and $K_{II} = 0$ criteria with the predefined crack path based on experimental observation [26].	61
Figure 4.1: Fretting fatigue loading arrangement [24].	62
Figure 4.2: Specimen and fretting pads (all dimensions in mm) [24].	63
Figure 4.3: Friction force vs Normal load[24].	65
Figure 4.4: Number of cycles for fretting failure versus contact pressure[24].	67
Figure 4.5: Crack length versus fatigue cycle ratio for axial load (a) 70MPa, (b) 100MPa, and (c) 125MPa[24].	68
Figure 4.6: Crack Propagation rate versus crack length for normal stress of (a) 20MPa, (b) 80MPa, and (c) 120MPa[24].	70
Figure 4.7: The influence of pad span on crack propagation rate versus crack length[24].	71
Figure 4.8: Fretting crack location and path[24].	72
Figure 5.1: Framework for the model developed for total life prediction in fretting fatigue	75
Figure 5.2: Node Penetration due to sharp edge	77
Figure 5.3: Effect of cycle jumping on SWT value for a specimen with axial stress = 100 MPa and Normal stress = 80 MPa	78
Figure 5.4: Variation of the SWT parameter with depth measured from the surface for a specimen with axial stress of 100MPa and Normal Stress of 80MPa.	80
Figure 5.5: Schematic description of the averaging method used for obtaining an average value of the SWT parameter.	81
Figure 5.6: Example of $\sigma_{\theta\theta}$ value over 180° range	82
Figure 5.7: Location of crack initiation.	83
Figure 5.8: (a) Single edge crack and (b) Double edge crack	84
Figure 6.1: Finite element model of a quarter of the fretting specimen-pad arrangement.	86
Figure 6.2: Normal load and cyclic axial load history applied to the finite element model.	86
Figure 6.3: Strain-Life Curves for 2014-T6/-T651[105].	87
Figure 6.4: Pressure distribution at the contact surface for different mesh sizes.	88



Figure 6.5: Comparison of theoretical contact pressure with simulation results.....	89
Figure 6.6: Variation of SWT parameter across the contact surface for different applied normal loads and axial stress of 100 MPa.....	91
Figure 6.7: Variation of SWT parameter across the contact surface for different applied normal loads for the axial stress of 100 MPa and a fixed COF value.....	91
Figure 6.8: Typical Contact Pressure distribution across the contact surface during compressive and tensile loading.....	92
Figure 6.9: Residual stress in the specimen with the axial stress of 100MPa and a normal load of 80MPa.....	93
Figure 6.10: Variation of normal and shear strain amplitudes and maximum stress across the contact surface for a specimen with axial stress of 100 MPa and contact stress of 80 MPa.....	95
Figure 6.11: Evolution of SWT parameter with loading cycles across the contact surface.....	96
Figure 6.12: Evolution of FS parameter with loading cycles across the contact surface.....	97
Figure 6.13: Evolution of SWT parameter with applied load cycles across the contact surface.....	99
Figure 6.14: Comparison of elastic plastic and wear models with different averaging size for predicting crack initiation.....	100
Figure 6.15: Effect of averaging size on crack initiation prediction.....	102
Figure 7.1: Comparison of crack path observed in the experimental work and predicted by FEM using MTS and $\Delta$ MTS criteria.....	106
Figure 7.2: Variation of $K_I$ with crack length along crack paths predicted by MTS and $\Delta$ MTS criteria and its comparison with experiments.....	107
Figure 7.3: Variation of plastic zone size ( $r_p$ ) at the crack tip with crack length for different normal stress values and the applied axial stress of: (a) 70 MPa, (b) 100 MPa, (c) 125 MPa.....	109
Figure 7.4: $\Delta K_I$ predicted for different axial and normal loads using LEFM approach....	110
Figure 7.5: $\Delta K_{eq}$ predicted for different axial and normal loads using a combined LEFM - EPFM approach.....	111
Figure 7.6: Crack propagation rates for a specimen with different normal loads and the applied axial stress of 70 MPa.....	113
Figure 7.7: Crack propagation rates for a specimen with different normal loads and the applied axial stress of 100 MPa.....	114

Figure 7.8: Crack propagation rates for a specimen with different normal loads and the applied axial stress of 125 MPa. ....	115
Figure 7.9: Predicted number of cycles of crack propagation for specimen with different normal loads and the applied axial stress of 70 MPa. ....	117
Figure 7.10: Predicted number of cycles of crack propagation for specimen with different normal loads and the applied axial stress 100 MPa. ....	118
Figure 7.11: Predicted number of cycles of crack propagation for specimen with different normal loads and the applied axial stress 125 MPa. ....	119
Figure 7.12: Variation of maximum stress intensity factor with crack length for single and double edge cracks. ....	120
Figure 7.13: Total lifetimes for specimen with axial stress of 100 MPa using single edge and double edge crack models. ....	121
Figure 7.14: Prediction of total fretting fatigue lifetimes and their comparison with the experimental data. ....	121

## List of Tables

Table 4.1 Materials Properties[24].....	63
Table 4.2 Experimental parameters[24].....	64
Table 4.3 Crack path data[24].....	72
Table 6.1 Crack nucleation prediction by linear elastic models .....	90
Table 6.2 Crack nucleation prediction by elastic-plastic model. ....	93
Table 6.3 Crack nucleation predictions by the elastic-plastic model including wear. ....	98
Table 6.4 Crack nucleation predictions by the averaging methods. ....	103

## **Abstract**

Nucleation and propagation of cracks under fretting conditions has been a subject of study for many years. An extensive experimental investigation to study these cracks was undertaken by Royal Aerospace Establishment (RAE Farnborough). Of particular interest to RAE was an Aluminium alloy (L65) developed for aerospace applications.

Many researchers have studied fretting damage and fatigue cracks. Some have examined damage development due to wear, whilst others have analysed cracks under linear elastic fracture mechanics (LEFM) domain. To date, no attempt has been made to develop an integrated numerical model which incorporates all aspects of fretting fatigue i.e. nucleation, initial (or early) crack growth, and long crack propagation. The development of such a model is the principal aim of this work. It is expected that the integrated approach will provide the basis for a standard fretting fatigue analysis of other materials, components, and structures using the finite element method (FEM).

This study uses the earlier experimental results with RAE as the reference for comparison. The approach followed is to implement the various stages of fretting in a commercial finite element code, ABAQUS. Unlike previously used simple FE models, both specimen (Aluminium alloy) and the fretting pad (steel) are modelled to simulate the real contact conditions including slip.

Various predictive models for crack nucleation (based on damage) and propagation (based on fracture mechanics) are developed, tested, and implemented in ABAQUS. Results clearly show that these models together provide a good estimation tool for predicting total life in complete contact fretting fatigue. It is envisaged that the integrated model will be easily utilised for other materials, components, and structures subjected to fretting fatigue conditions with minimum experimental testing required.

## **Declaration**

No portion of the work referred to in the thesis has been submitted in support of an application for another degree or qualification of this or any other university or other institute of learning.

Mohamad Haidir Maslan

January 2016

## Copyright Statement

- i. The author of this thesis (including any appendices and/or schedules to this thesis) owns certain copyright or related rights in it (the “Copyright”) and s/he has given The University of Manchester certain rights to use such Copyright, including for administrative purposes.
- ii. Copies of this thesis, either in full or in extracts and whether in hard or electronic copy, may be made only in accordance with the Copyright, Designs and Patents Act 1988 (as amended) and regulations issued under it or, where appropriate, in accordance with licensing agreements which the University has from time to time. This page must form part of any such copies made.
- iii. The ownership of certain Copyright, patents, designs, trademarks and other intellectual property (the “Intellectual Property”) and any reproductions of copyright works in the thesis, for example graphs and tables (“Reproductions”), which may be described in this thesis, may not be owned by the author and may be owned by third parties. Such Intellectual Property and Reproductions cannot and must not be made available for use without the prior written permission of the owner(s) of the relevant Intellectual Property and/or Reproductions.
- iv. Further information on the conditions under which disclosure, publication and commercialisation of this thesis, the Copyright and any Intellectual Property and/or Reproductions described in it may take place is available in the University IP Policy (see <http://documents.manchester.ac.uk/DocuInfo.aspx?DocID=487>), in any relevant Thesis restriction declarations deposited in the University Library, The University Library’s regulations (see <http://www.manchester.ac.uk/library/aboutus/regulations>) and in The University’s policy on Presentation of Theses

## **Acknowledgements**

First and foremost, I would like to express my sincerest gratitude to my supervisor, Dr Mohammad Sheikh who has giving me guidance, support and inspiration throughout my PhD programme. Without his patient, kind and assistance, the completion of this thesis would not have been possible.

Many special thanks go to The Ministry of Education Malaysia and Universiti Teknikal Malaysia Melaka (UTeM) as the sponsor of my tuition fees and provided the financial support during my research years in Manchester.

I would like to thank to all technical staffs in The University of Manchester that may have given direct and indirect support in completing various stages of this research. Not forget to mention supportive colleagues especially those in Floor D and F of Pariser Building that always keen to help each other in completing our courses

I could not have thanks enough for the moral support and unconditional love given by my parents, Maslan Isa and Kaujah Yahok. Thanks for all the financial backings that they have given me.

Finally, I wish to thank my lovely wife, Noraini Kurdi. Her understanding towards the challenges faced by me, her patience and supports were very much needed and tremendously appreciated. Thank you to all my kids, Nazurah Hana, Muhammad Taqiuddin, and Muadz Daniel for always cheering me up during all this period.

Thank you to everyone who at some point has contributed any means of support during the course of my PhD. I am forever in your debt.

## Nomenclature

### Acronyms

ASTM	American Society for Testing and Materials
$\Delta MTS$	Maximum Tangential Stress Range
EPFM	Elastic-Plastic Fracture Mechanics
FEM	Finite Element Method
FS	Fatemi-Socie
LEFM	Linear Elastic Fracture Mechanics
MERR	Maximum Energy Release Rate
MTS	Maximum Tangential Stress
NTSB	National Transportation Safety Board
SWT	Smith-Watson-Topper

### Roman Symbols

$a$	semi contact width
$B$	Specimen thickness
$b$	fatigue strength exponent
$c$	fatigue durability exponent
$D$	damage fraction
$R$	Cylinder radius
$2D$	two dimensional
$P$	Normal Load (N)
$E$	Young Modulus (MPa)
$E^*$	combined modulus (MPa)
$F_{friction}$	Friction load (N)



H	Hardness
$J$	Strain energy release rate or work input rate ( $J/m^2$ )
$K_I, K_{II}, K_{III}$	Mode I, II, and III stress intensity factors ( $MPa\sqrt{m}$ )
$K_{IC}$	Plane strain fracture toughness ( $MPa\sqrt{m}$ )
N	Normal load (N)
$N_f$	Life (cycle to failure)
P	contact pressure (MPa)
$p(x)$	contact pressure (MPa)
$p_o$	maximum normal pressure (MPa)
$r_p$	Plastic zone size ( $\mu m$ )
S	Sliding distance ( $\mu m$ )
W	rate of wear ( $m^3/m$ )
$W_s$	Work required to create new surfaces

### Greek Symbols

$\nu$	Poisson Ratio
$\mu$	coefficient of friction
$\varepsilon_a$	strain amplitude
$\varepsilon_{ea}$	elastic strain amplitude
$\varepsilon_{pa}$	plastic strain amplitude
$\varepsilon_f'$	fatigue ductility coefficient
$\gamma$	shear strain
$\sigma_a$	normal stress amplitude (MPa)
$\sigma_f'$	fatigue strength coefficient (MPa)
$\sigma_{xx}, \sigma_{yy}, \tau_{xy}$	2-D stress components in Cartesian Coordinates (MPa)

$\sigma_{rr}, \sigma_{\theta\theta}, \tau_{r\theta}$	2-D stress components in Polar Coordinates (MPa)
$\sigma_y$ or $\sigma_{ys}$	Yield Stress (MPa)
$\sigma_{max}$	maximum stress (MPa)
$\tau$	shear stress (MPa)
$\theta$	direction in front crack tip

## CHAPTER 1. INTRODUCTION

### 1.1 Introduction

Fatigue failure was detected as early as 1837. Despite many attempts that have been made to understand and to avoid accidents due to fatigue failure, these failures still continue to occur. In the aircraft industry for example, fatigue failure was the cause of catastrophic accident of the first commercial aircraft de Havilland Comet in 1953[1]. Three aircrafts broke up during mid-flight within one year after the commercial aircraft was launched. Investigations indicated that the main cause of these catastrophic failures was by metal fatigue in the airframes. Windows with sharp corners followed by rivet holes around increased the stress concentration, as shown in Figure 1.1. Lack of knowledge about fatigue at the time contributed to this rather inferior design. These accidents, however, led the company and the competitors to invest more on research on metal fatigue resulting in better and safe design of aircrafts.

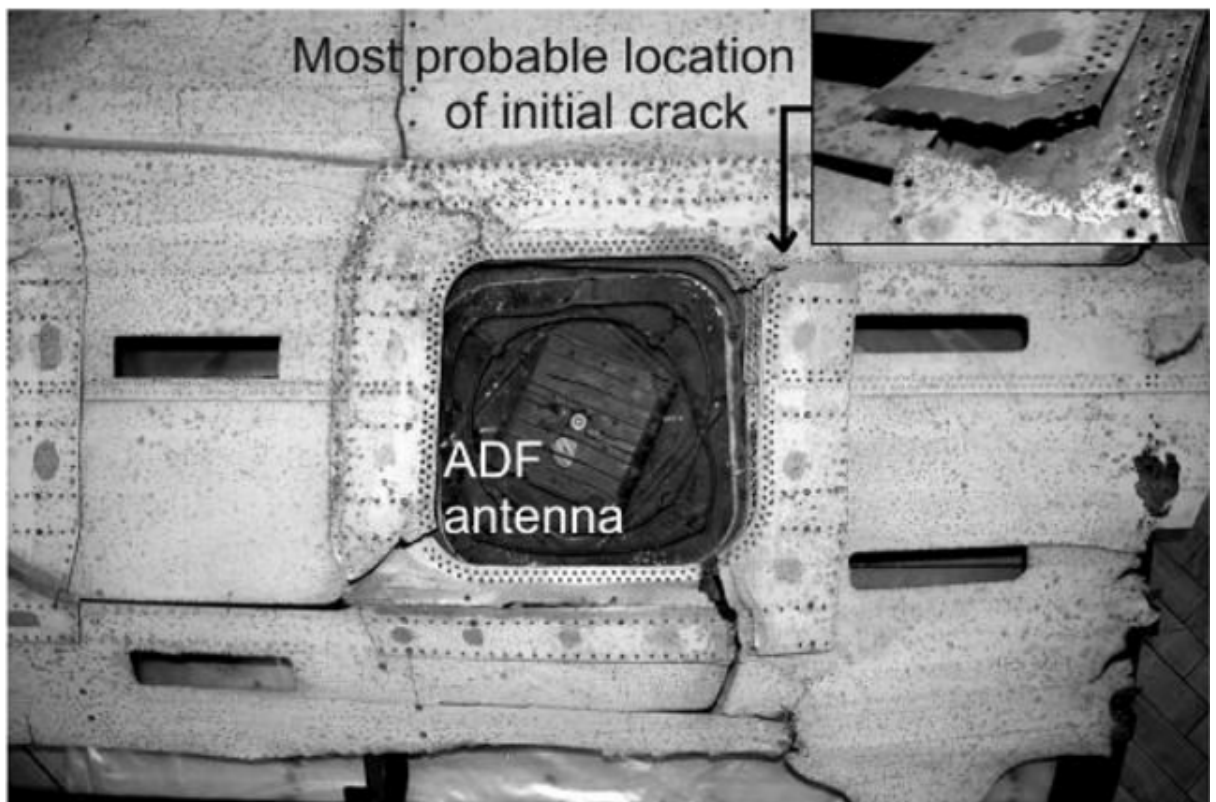


Figure 1.1: Fuselage fragment of Comet [2].

## Introduction

Despite improvements, another fatigue failure involving a rivet joint occurred 35 years later in 1988. A Boeing 737-200 owned by Aloha Airlines, experienced an explosive decompression due to mechanical structural failure during flight. Approximately 5.5 m of the cabin skin and structure of the cabin entrance door above the passenger floor had separated from the aircraft (Figure 1.2).



Figure 1.2: Aloha Airline flight 243 accident [3].

Failure was found to have initiated along a fuselage skin longitudinal lap joint that had been cold bonded and also contained three rows of additional countersunk rivets. Fuselage hoop loads were intended to be transferred through the joint rather than through the rivets. However, some areas of the lap joints did not bond at all, the hoop load transfer through the joint was borne by the three rows of countersunk rivets. The countersinking extended through the entire thickness of the sheet which resulted in a knife edge being created at the bottom of the hole, as shown in Figure 1.3. Stress concentrated at the knife edge and promoted fatigue crack nucleation. For this reason, fatigue cracking began in the outer layer of the skin at a lap joint along the upper and highly stressed row of rivet holes.

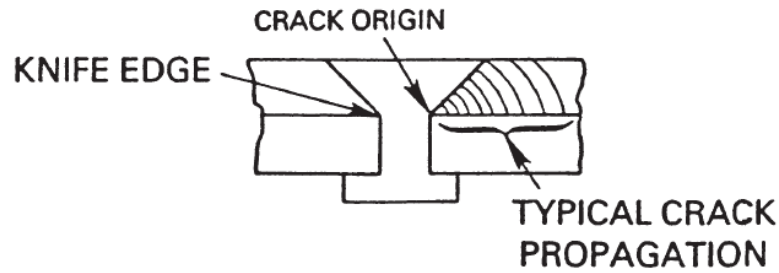


Figure 1.3: Schematic view of a countersunk rivet and the associated fatigue crack observed in Aloha Airlines 737 accident [3]

More recently, in April 2011, a Boeing 737 operating for Southwest Airlines [3] experienced a rapid decompression during flight. The aircraft sustained substantial damage; post-accident inspection revealed that a section of fuselage skin had fractured and flapped open on the upper left side above the wing, Figure 1.4. The entire section of skin remained attached along the lower edge and was deformed outward, as shown in Figure 1.5. The fracture along the upper edge was through the lower rivet row of the lap joint. There was no visible damage to the surrounding frames, stringers, and stringer clips. At National Transportation Safety Board (NTSB) materials laboratory, microscopic examination of the fracture surfaces of the ruptured skin revealed fatigue cracks emanating from at least 42 out of the 58 rivet holes. Non-destructive eddy current inspections were conducted around the intact rivets on the removed skin section forward of the rupture revealed indications of cracks at nine rivet holes in the lower rivet row of the lap joint.



Figure 1.4: Photograph of Southwest airliner with a hole in the upper left fuselage [4]

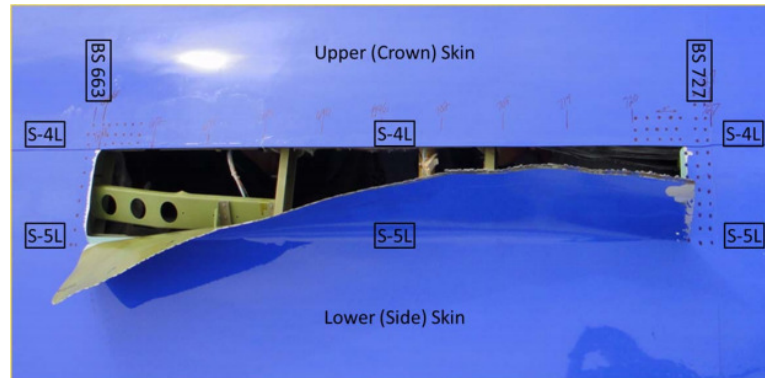


Figure 1.5: Close-up view of the hole in the fuselage side skin [4]

According to NTSB technical report [4], at the inner surface of the lap joint, the rivet holes in the upper and lower skins were found to be slightly offset relative to each other, and many of the rivet holes on the lower skin were not circular but slightly oval. The fracture (fatigue cracks) intersected the majority of the lower-row rivet holes. The corresponding area located at the underside of the expanded portion of the rivets also showed fretting damage consistent with the underside of the expanded portion of the shank rubbing against the plate.

With this simple example, it can be concluded that continuous in-depth study of each accident is necessary. Although accidents may be unavoidable, design improvements can hopefully reduce the chance for such accidents to occur.

### 1.2 Fretting Fatigue

Fretting is a rubbing process between two surfaces due to oscillatory micro-slip which occurs between them. It occurs in machine components subjected to a clamping pressure and vibratory excitation or an oscillatory tangential force. Fretting damage can be classified into fretting fatigue and fretting wear.

Fretting wear is the result of repeated fretting between two surfaces over a period of time which will remove material from one or both surfaces in contact. In fretting wear, damage is measured by the volumetric material loss.

Fretting fatigue, on the other hand, is defined in terms of the reduction in fatigue strength or fatigue life due to small amplitude movement between contacting surfaces as one of the members is subjected to a cyclic stress.



Fretting fatigue is common in many mechanical systems and engineering structures (for example: aircrafts, spacecrafts, automobile, electrical equipment, manufacturing equipment, human body implants, etc.) which are subjected to variable cyclic loading on the components in contact. There are many practical applications that are subjected to fretting fatigue, such as bolted and riveted connections, bearing shafts, blade-disk attachment in gas and steam turbines and aero-engine splined couplings.

Figure 1.6 shows two examples of fretting fatigue in aircraft machinery components.

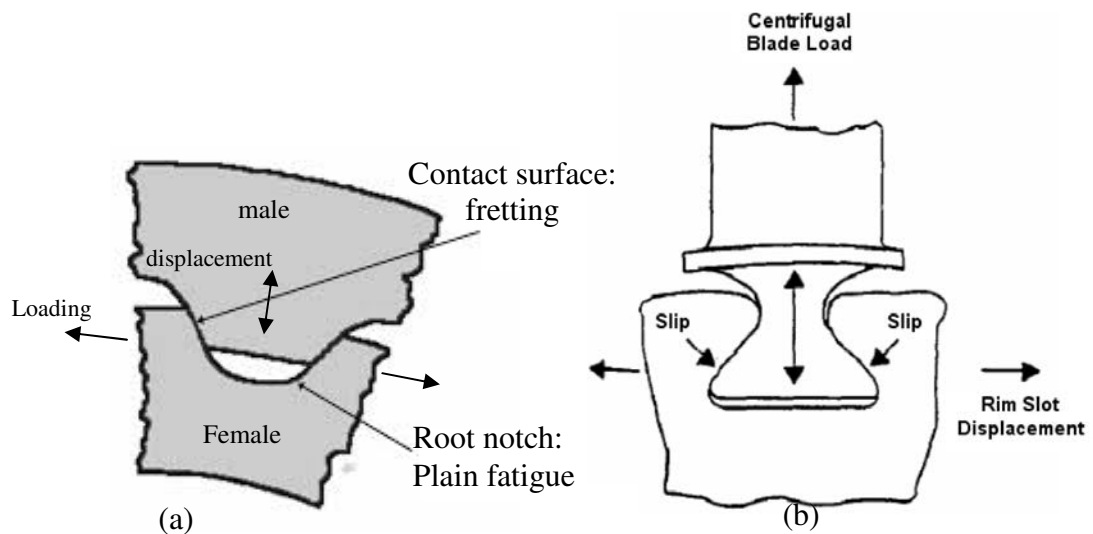


Figure 1.6: fretting fatigue on (a) spline coupling (b) dovetail joint.

### 1.3 Previous Research

Most of previous fretting fatigue studies have been carried out for aerospace applications where weight and strength are main concerns. The most extensively studied materials are aluminium and titanium alloys as they are used for aerospace structures and engine parts. In the experimental work, these materials are studied in either a bridge or a single pad configuration in complete or incomplete fretting contact. Experimental studies are also carried out on actual components such as rivet joints, dovetail joints and spline couplings.

Besides experimental work, fretting fatigue is also studied using computer simulations. Finite element methods are used to investigate in detail stress, slip, and several other parameters which affect fatigue life. FEM is also used to model crack initiation and propagation in fretting fatigue using critical plane analysis and fracture mechanics. Wear

## Introduction

surface profiles affected by adhesive wear and plastic ratcheting can also be modelled with FEM.

Despite the extensive experimental and modelling work which has been carried out previously on fretting fatigue, it has concentrated mainly on incomplete contact and complete contact has largely been ignored. Although the two types of contact have many similarities, there are several characteristics of complete contact with sharp edges which can cause different tribological effects. Hence, this study intends to include tribological parameters such as wear to improve the current state of complete contact fretting fatigue modelling.

### 1.4 Overall Aim and Objectives

The ultimate aim of this research is to develop a modelling methodology for predicting fretting fatigue life which includes the tribological aspects of fretting.

The specific objectives are:

- To model fretting crack initiation which includes evolution of surface profile and surface degradation due to wear.
- To model fatigue crack growth of a short crack until fracture by considering multiaxial effects.
- To integrate all the models to produce a total fretting life model in fretting fatigue.

### 1.5 Structure of report

Following the introduction (**Chapter 1**), this report is divided into the following chapters:

#### **Chapter 2 Parameters in Fretting Fatigue**

This chapter presents a fundamental understanding of the parameters associated with fretting fatigue. It includes contact mechanics, tribology, fatigue, and fretting fatigue.

#### **Chapter 3 Literature Review**

This chapter presents a literature review on previous relevant works, discussing state of the art in the field according to scope of this thesis. It consists of contact and failure mechanics